

# Constraints on the anomalous tensor operators from $B \rightarrow \phi K^*, \eta K^*$ and $\eta K$ decays

Qin Chang<sup>ab</sup>, Xin-Qiang Li<sup>cd</sup>, Ya-Dong Yang<sup>a</sup>

<sup>a</sup> Institute of Particle Physics, Huazhong Normal University, Wuhan, Hubei 430079, P. R. China

<sup>b</sup> Department of Physics, Henan Normal University, Xinxiang, Henan 453007, P. R. China

<sup>c</sup> Institute of Theoretical Physics, Chinese Academy of Sciences, Beijing, 100080, P. R. China

<sup>d</sup> Graduate School of the Chinese Academy of Sciences, Beijing, 100039, P. R. China

E-mail: changqin1981@163.com, xqli@itp.ac.cn, yangyd@iopp.ccnu.edu.cn

July 3, 2018

## Abstract

We investigate whether the anomalous tensor operators with the Lorentz structure  $\sigma_{\mu\nu}(1 + \gamma_5) \otimes \sigma^{\mu\nu}(1 + \gamma_5)$ , which could provide a simple resolution to the polarization anomaly observed in  $B \rightarrow \phi K^*$  decays, could also provide a coherent resolution to the large  $\mathcal{B}(B \rightarrow \eta K^*)$  and survive bounds from  $B \rightarrow \eta K$  decays. Parameter spaces satisfying all these experimental data are obtained, and found to be dominated by the color-octet tensor operator contribution. Constraints for the equivalent solution with  $(1 + \gamma_5) \otimes (1 + \gamma_5)$  operators are also derived and found to be dominated by the color-singlet one. With the constrained parameter spaces, we finally give predictions for  $B_s \rightarrow \phi\phi$  decay, which could be tested at the Fermilab Tevatron and the LHC-b experiments.

PACS Numbers: 13.25.Hw, 12.38.Bx, 12.15.Mm.

# 1 Introduction

Looking for signals of physics beyond the Standard Model (SM) is one of the most important missions of high energy physics. Complementary to direct searches for new physics (NP) particles in the high energy colliders, the study of  $B$  physics is of great importance for probing indirect signals of NP. In this respect, the  $B$  factories at SLAC and KEK are doing a commendable job by providing us with a huge amount of data on various  $B$ -meson decays, which are mostly in perfect agreement with the SM predictions. However, there still exist some unexplained puzzles, such as the unmatched  $CP$  asymmetries in  $B \rightarrow \pi K$  decays [1, 2, 3], the abnormally large branching ratios of  $B \rightarrow \eta' K$  and  $B \rightarrow \eta K^*$  decays [1, 2, 4, 5, 6, 7, 8, 9, 10], and the large transverse polarization fractions in  $B \rightarrow \phi K^*$  decays [1, 2, 11, 12, 13, 14, 15, 17, 18, 19, 20]. Confronted with these anomalies, we are forced not only to consider more precise QCD effects, but also to speculate on the existence of possible NP scenarios beyond the SM.

It is well-known that the flavor-changing neutral current (FCNC) processes arise only from loop effects within the SM, and are therefore very sensitive to various NP effects. Since the puzzling  $B$ -meson decay processes mentioned above are all related to the FCNC  $b \rightarrow s$  transitions, these decay channels could be used as effective probes of possible NP scenarios. So, if one kind of NP could resolve one of these puzzles, it is necessary to investigate whether the same scenario can also provide a simultaneous resolution to the others. Considering the fact that current theoretical estimations of  $\mathcal{B}(B \rightarrow \eta' K)$  still suffer from large uncertainties [9, 21], and the NP scenario with anomalous tensor operators considered in this paper do not contribute to the  $B \rightarrow \phi K$  and  $B \rightarrow \pi K$  decays in the naive factorization (NF) approximation, we shall only focus on the  $B \rightarrow \eta K^{(*)}$  and  $B \rightarrow \phi K^*$  decays.

The recent experimental data on the longitudinal polarization fraction  $f_L$  in  $B^0 \rightarrow \phi K^{*0}$  decay is given as

$$f_L = \begin{cases} 0.52 \pm 0.05 \pm 0.02 & \text{BABAR [11],} \\ 0.45 \pm 0.05 \pm 0.02 & \text{Belle [12],} \\ 0.57 \pm 0.10 \pm 0.05 & \text{CDF [13].} \end{cases} \quad (1)$$

On the other hand, since the two final-state light vector mesons  $\phi$  and  $K^{*0}$  in this decay mode are flying out fleetly in the rest frame of  $B$  meson, and the structure of the charged weak interaction current of the SM is left-handed, as well as the fact that high-energy QCD

interactions conserve helicity, any spin flip of a fast flying quark will be suppressed by one power of  $1/m_b$ , with  $m_b$  the  $b$  quark mass. It is therefore expected that, within the SM, both of the final-state hadrons in this decay mode are mainly longitudinally polarized, with

$$f_L \sim 1 - \mathcal{O}(1/m_b^2), \quad (2)$$

while the transverse parts are suppressed by powers of  $m_{\phi, K^*}/m_B$ . Obviously, the experimental data Eq. (1) deviates significantly from the SM prediction Eq. (2), and this polarization anomaly has attracted much interest in searching for possible theoretical explanations both within the SM and in various NP models [14, 17, 18, 19, 20]. For example, the authors in Refs. [17, 18, 19, 20] have studied this anomaly and found that the four-quark tensor operators of the form  $\bar{s}\sigma_{\mu\nu}(1+\gamma_5)b \otimes \bar{s}\sigma^{\mu\nu}(1+\gamma_5)s$  could offer a simple resolution to the observed polarization anomaly within some possible parameter spaces.

Since the  $B \rightarrow \eta K^{(*)}$  decays, in analogy with the  $B \rightarrow \phi K^*$  decays, also involve the  $b \rightarrow s\bar{s}s$  transition, it is necessary to investigate the effects of these new types of four-quark tensor operators on the latter. In particular, it is very interesting to see whether these new four-quark tensor operators with the same parameter spaces could also simultaneously account for the measured  $\mathcal{B}(B \rightarrow \eta K^*)$  [2, 4, 5, 6], which are much larger than the theoretical predictions within the SM [8, 9], and survive bounds from  $B \rightarrow \eta K$  decays. Motivated by these speculations, in this paper, we shall investigate the effects of the following two types of tensor operators on these decay modes (with  $i, j$  the color indices)

$$O_{T1} = \bar{s}\sigma_{\mu\nu}(1+\gamma_5)b \otimes \bar{s}\sigma^{\mu\nu}(1+\gamma_5)s, \quad O_{T8} = \bar{s}_i\sigma_{\mu\nu}(1+\gamma_5)b_j \otimes \bar{s}_j\sigma^{\mu\nu}(1+\gamma_5)s_i, \quad (3)$$

and try to find out the allowed parameter spaces characterized by the strengths and phases of these new tensor operators that satisfy all the experimental constraints from these decays. Moreover, since the (pseudo-)scalar operators

$$O_{S+P} = \bar{s}(1+\gamma_5)b \otimes \bar{s}(1+\gamma_5)s, \quad O'_{S+P} = \bar{s}_i(1+\gamma_5)b_j \otimes \bar{s}_j(1+\gamma_5)s_i, \quad (4)$$

can be expressed, through the Fierz transformations, as linear combinations of the new tensor operators Eq. (3), constraints on these two operators can be derived easily from those on the latter.

To further test such a particular NP scenario with anomalous tensor operators, we also give predictions for the branching ratio and the longitudinal polarization fraction of  $B_s \rightarrow \phi\phi$  decay, which is also involved the same quark level  $b \rightarrow s\bar{s}s$  transition. All these results could be tested at the Fermilab Tevatron and the LHC-b experiments.

The paper is organized as follows. Sec. 2 is devoted to the theoretical framework. After a brief entertainment of the QCD factorization formalism (QCDF) [22], we discuss the anomalous tensor operator contributions to the  $B \rightarrow \eta K^{(*)}$  and  $B \rightarrow \phi K^*$  decays. In Sec. 3, our numerical analysis and discussions are presented. Sec. 4 contains our conclusions. Appendix A recapitulates the amplitudes for the five decay modes within the SM [15, 23]. All the theoretical input parameters relevant to our analysis are summarized in Appendix B.

## 2 Theoretical Framework

### 2.1 The SM results within the QCDF framework

In the SM, the effective Hamiltonian responsible for  $b \rightarrow s$  transitions is given as [24]

$$\begin{aligned} \mathcal{H}_{\text{eff}} = & \frac{G_F}{\sqrt{2}} \left[ V_{ub}V_{us}^* (C_1 O_1^u + C_2 O_2^u) + V_{cb}V_{cs}^* (C_1 O_1^c + C_2 O_2^c) - V_{tb}V_{ts}^* \left( \sum_{i=3}^{10} C_i O_i \right. \right. \\ & \left. \left. + C_{7\gamma} O_{7\gamma} + C_{8g} O_{8g} \right) \right] + \text{h.c.}, \end{aligned} \quad (5)$$

where  $V_{qb}V_{qs}^*$  ( $q = u, c$  and  $t$ ) are products of the Cabibbo-Kobayashi-Maskawa (CKM) matrix elements [25],  $C_i$  the Wilson coefficients, and  $O_i$  the relevant four-quark operators whose explicit forms could be found, for example, in Ref. [22].

In addition to  $\mathcal{H}_{\text{eff}}$ , we must employ a factorisation formalism of hadronic dynamics to study the  $B^- \rightarrow \eta K^-$ ,  $\bar{B}^0 \rightarrow \eta \bar{K}^0$ ,  $B^- \rightarrow \eta K^{*-}$ ,  $\bar{B}^0 \rightarrow \eta \bar{K}^{*0}$ , and  $\bar{B}^0 \rightarrow \phi \bar{K}^{*0}$  decays. To this end, we take the framework of QCDF [22]. The factorization formula allows us to calculate systemically the hadronic matrix element of operators in the effective Hamiltonian Eq. (5)

$$\begin{aligned} \langle M_1 M_2 | O_i | B \rangle = & \sum_j F_j^{B \rightarrow M_1} \int_0^1 dx T_{ij}^I(x) \Phi_{M_2}(x) + (M_1 \leftrightarrow M_2) \\ & + \int_0^1 d\xi \int_0^1 dx \int_0^1 dy T_i^{II}(\xi, x, y) \Phi_B(\xi) \Phi_{M_1}(x) \Phi_{M_2}(y), \end{aligned} \quad (6)$$

where  $F_j^{B \rightarrow M}$  is the  $B \rightarrow M$  transition form factor,  $T_{ij}^I$  and  $T_i^{II}$  are the perturbatively calculable hard kernels, and  $\Phi_X(x)$  ( $X = B, M_{1,2}$ ) are the universal nonperturbative light-cone distribution amplitudes (LCDAs) of the corresponding mesons.

In the recent years, the QCDF formalism has been employed extensively to study non-leptonic  $B$  decays. For example, all the decay modes considered here have been studied comprehensively within the SM in Refs. [15, 23]. We recapitulate the amplitudes for  $B \rightarrow \eta K^{(*)}$  and  $B \rightarrow \phi K^*$  decays in Appendix A.

It is noted that, along with its many novel progresses in non-leptonic  $B$  decays, the framework contains estimates of some power corrections which can not be computed rigorously. These contributions may be numerically important for realistic  $B$ -meson decays, especially for some penguin-dominated decay modes [15, 17, 23, 26]. In fact, there are no reliable methods available at present to *calculate* such contributions. To give *conservative* theoretical predictions, at least, one should leave the associated parameters varying in reasonable regions to show their possible effects. In this work, following closely the treatment made in Refs. [23, 27], we will parameterize the end-point divergences associated with these power corrections as

$$\int_0^1 \frac{dx}{x} \rightarrow X_A = e^{i\phi_A} \ln \frac{m_B}{\Lambda_h}, \quad \int_0^1 \frac{dx}{x^2} \rightarrow X_L = \frac{m_B}{\Lambda_h} e^{i\phi_A} - 1. \quad (7)$$

In the following numerical calculations, we take the parameter  $\Lambda_h$  and the phase  $\phi_A$  varying in the range  $0.2 \sim 0.8$  GeV and  $-45^\circ \sim 45^\circ$ , respectively.

In our calculation, we have neglected possible intrinsic charm content and anomalous gluon couplings related to the meson  $\eta$ , both of which have been shown to have only marginal effects on the four  $B \rightarrow \eta K^{(*)}$  decays [8, 9]. As for the  $\eta$ - $\eta'$  mixing effects, we shall adopt the Feldmann-Kroll-Stech (FKS) scheme [28] as implemented in Ref. [9]. A recent study and comparison of different  $\eta$ - $\eta'$  mixing schemes has been given in Ref. [29].

In the amplitude for  $\bar{B}^0 \rightarrow \phi \bar{K}^*$  decay in Eq. (39), a new power-enhanced electromagnetic penguin contribution to the negative-helicity electroweak penguin coefficient  $\alpha_{3,\text{EW}}^{p,-}$ , as first noted by Beneke, Rohrer and Yang [15], has also been taken into account in our calculation. In a recent comprehensive study of  $B \rightarrow VV$  decays [16], it is found that the small  $f_L$  could be accommodated within the SM, however, with very large theoretical uncertainties.

## 2.2 Anomalous tensor operators and their contributions to the decay amplitudes

Since the SM may have difficulties in explaining the large  $\mathcal{B}(B \rightarrow \eta K^*)$  and the measured polarization observables in  $B \rightarrow \phi K^*$  decays, we shall discuss possible NP resolutions to these observed discrepancies. Specifically, we shall investigate whether these discrepancies could be resolved by introducing two anomalous four-quark tensor operators defined by Eq. (3).

We write the NP effective Hamiltonian as

$$\mathcal{H}_{eff}^{\text{NP}} = \frac{G_F}{\sqrt{2}} |V_{ts}| e^{i\delta_T} \left[ C_{T1} O_{T1} + C_{T8} O_{T8} \right] + \text{h.c.}, \quad (8)$$

with the tensor operators  $O_{T1}$  and  $O_{T8}$  defined by Eq. (3). The coefficient  $C_{T1(T8)}$  describes the relative interaction strength of the tensor operator  $O_{T1(T8)}$ , and  $\delta_T$  is the NP weak phase. In principle, such four-quark tensor operators could be produced in various NP scenarios, e.g., in the Minimal Supersymmetric Standard Model (MSSM) [30, 31]. Interestingly, the recent study of radiative pion decay  $\pi^+ \rightarrow e^+ \nu \gamma$  at PIBETA detector [32] has found deviations from the SM predictions in the high- $E_\gamma$ -low- $E_{e^+}$  kinematic region, which may indicate the existence of anomalous tensor quark-lepton interactions [33, 34, 35].

At first, we present the NP contributions to the decay amplitudes of  $B \rightarrow \eta K^{(*)}$  and  $B \rightarrow \phi K^*$  decays due to these new tensor operators. Since their coefficients are unknown parameters, for simplicity, we shall only consider the leading contributions of these tensor operators.

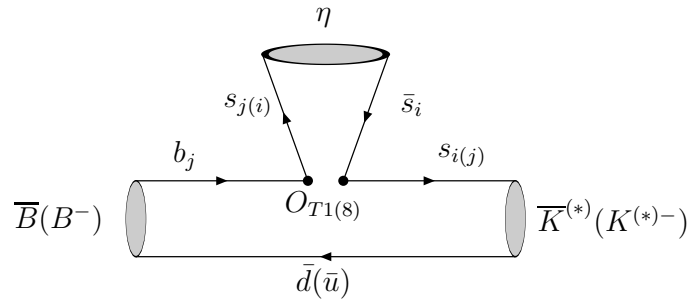


Figure 1: Feynman diagram contributing to the decay amplitudes of  $B \rightarrow \eta K^{(*)}$  decays due to the anomalous tensor operators. Another type of insertion has no contribution.

As for the four  $B \rightarrow \eta K^{(*)}$  decays, the relevant Feynman diagram due to the tensor operators  $O_{T1,T8}$  is shown in Fig. 1. It is easy to realize that the amplitude corresponding to

another type of insertion would vanish in the leading order approximation. Instead of using the Fierz transformation, an easy way to calculate the amplitude in Fig. 1 is to use the light-cone projection operator of the meson  $\eta$  in momentum space [23]

$$M_{\alpha\beta}^{\eta_s} = \frac{if_\eta^s}{4} \left[ \not{q} \gamma_5 \Phi_\eta(x) - \mu_{\eta_s} \gamma_5 \frac{k_2^\mu k_1^\mu}{k_2 \cdot k_1} \Phi_p(x) \right]_{\alpha\beta}, \quad (9)$$

where  $q$ ,  $\Phi_\eta$ , and  $\Phi_p$  are the momentum, leading-twist, and twist-3 LCDAs of the meson  $\eta$ , respectively.  $k_1^\mu$  and  $k_2^\mu$  denote the momenta of the quark and anti-quark in the meson  $\eta$ , and are given by

$$k_1^\mu = xq^\mu + k_\perp^\mu + \frac{\vec{k}_\perp^2}{2xq \cdot \bar{q}} \bar{q}^\mu, \quad k_2^\mu = \bar{x}q^\mu - k_\perp^\mu + \frac{\vec{k}_\perp^2}{2\bar{x}q \cdot \bar{q}} \bar{q}^\mu, \quad (10)$$

with  $\bar{x} = 1 - x$ , and  $x$  the momentum fraction carried by the constituent quark. The decay constant  $f_\eta^s$  and the factor  $\mu_{\eta_s}$  in Eq. (9) are defined, respectively, by [9]

$$\langle \eta(q) | \bar{s} \gamma_\mu \gamma_5 s | 0 \rangle = -if_\eta^s q_\mu, \quad \mu_{\eta_s} = \frac{\bar{m}_b}{2} r_\chi^{\eta_s} = \frac{h_\eta^s}{2f_\eta^s \bar{m}_s}, \quad (11)$$

where we have used  $|\eta\rangle = \cos\phi|\eta_q\rangle - \sin\phi|\eta_s\rangle$ , with  $|\eta_q\rangle = (|\bar{u}u\rangle + |\bar{d}d\rangle)/\sqrt{2}$  and  $|\eta_s\rangle = |\bar{s}s\rangle$  [28].

After some simple calculations, the NP contributions to the decay amplitudes of the four  $B \rightarrow \eta K^{(*)}$  decays due to  $\mathcal{H}_{eff}^{NP}$  in Eq. (8) can be written as

$$\mathcal{A}_{B^- \rightarrow \eta K^-}^{\text{NP}} = i \frac{G_F}{\sqrt{2}} |V_{ts}| e^{i\delta_T} 3 g_T r_\chi^{\eta_s} (m_{B_u}^2 - m_{K^-}^2) F_0^{B \rightarrow K}(m_\eta^2) f_\eta^s, \quad (12)$$

$$\mathcal{A}_{B^0 \rightarrow \eta \bar{K}^0}^{\text{NP}} = i \frac{G_F}{\sqrt{2}} |V_{ts}| e^{i\delta_T} 3 g_T r_\chi^{\eta_s} (m_{B_d}^2 - m_{K^0}^2) F_0^{B \rightarrow K}(m_\eta^2) f_\eta^s, \quad (13)$$

$$\mathcal{A}_{B^- \rightarrow \eta K^{*-}}^{\text{NP}} = -i \sqrt{2} G_F |V_{ts}| e^{i\delta_T} 3 g_T r_\chi^{\eta_s} m_{K^{*-}} (\varepsilon_2^* \cdot p) A_0^{B \rightarrow K^*}(m_\eta^2) f_\eta^s, \quad (14)$$

$$\mathcal{A}_{B^0 \rightarrow \eta \bar{K}^{*0}}^{\text{NP}} = -i \sqrt{2} G_F |V_{ts}| e^{i\delta_T} 3 g_T r_\chi^{\eta_s} m_{\bar{K}^{*0}} (\varepsilon_2^* \cdot p) A_0^{B \rightarrow K^*}(m_\eta^2) f_\eta^s, \quad (15)$$

where  $g_T = C_{T8} + C_{T1}/N_c$ , and the factor 3 is due to contractions of the involved  $\gamma$  matrices. It is interesting to note that the above four decay amplitudes are all proportional to the ‘‘chirally-enhanced’’ factor  $r_\chi^{\eta_s} = \frac{h_\eta^s}{f_\eta^s \bar{m}_b \bar{m}_s}$ , which has been found to be very important for charmless hadronic  $B$  decays [23].

We now present the NP contribution to the decay amplitude of  $\bar{B}^0 \rightarrow \phi \bar{K}^{*0}$  decay. Based on the observation that they contribute only to the transverse polarization amplitudes but not to the longitudinal one [17, 18, 19], these anomalous four-quark tensor operators have been proposed to resolve the polarization anomaly observed in  $B \rightarrow \phi K^*$  decays. The relevant

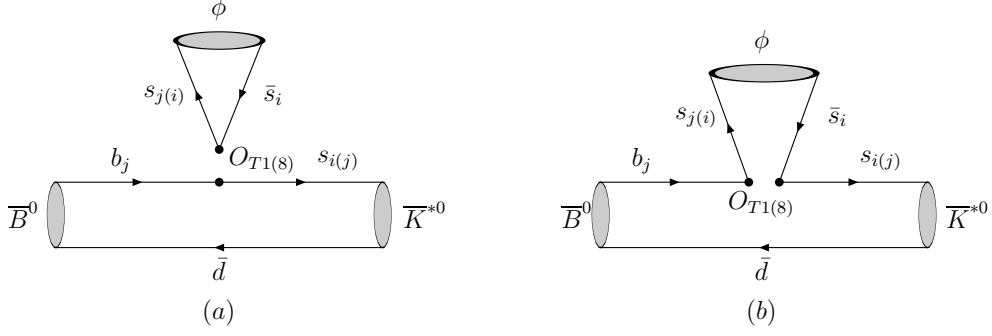


Figure 2: Feynman diagrams contributing to the decay amplitude of  $\bar{B}^0 \rightarrow \phi \bar{K}^{*0}$  decay due to the anomalous tensor operators.

Feynman diagrams are shown in Fig. 2. For Fig. 2 (a), we shall use the following matrix elements [36, 37, 38]

$$\langle \phi(q, \varepsilon_1) | \bar{s} \sigma^{\mu\nu} s | 0 \rangle = -f_\phi^T (\varepsilon_{1\perp}^{\mu*} q_\nu - \varepsilon_{1\perp}^{\nu*} q_\mu), \quad (16)$$

$$\langle \bar{K}^*(p', \varepsilon_2) | \bar{s} \sigma_{\mu\nu} q^\nu b | \bar{B}(p) \rangle = \epsilon_{\mu\nu\rho\sigma} \varepsilon_2^{*\nu} p^\rho p'^\sigma 2T_1^{B \rightarrow K^*}(q^2),$$

$$\begin{aligned} \langle \bar{K}^*(p', \varepsilon_2) | \bar{s} \sigma_{\mu\nu} q^\nu \gamma_5 b | \bar{B}(p) \rangle &= (-i) T_2^{B \rightarrow K^*}(q^2) \left\{ \varepsilon_{2,\mu}^* (m_B^2 - m_{K^*}^2) - (\varepsilon_2^* \cdot p) (p + p')_\mu \right\} \\ &+ (-i) T_3^{B \rightarrow K^*}(q^2) (\varepsilon_2^* \cdot p) \left\{ q_\mu - \frac{q^2}{m_B^2 - m_{K^*}^2} (p + p')_\mu \right\}. \end{aligned} \quad (17)$$

For Fig. 2 (b), we shall use the light-cone projector operator of the transversely polarized vector meson  $\phi$  [15, 36]

$$M_\perp^\phi = -\frac{i f_\phi^T}{4} \not{\varepsilon}_{1\perp}^* \not{q} \Phi_\perp(x) + \dots, \quad (18)$$

where  $\Phi_\perp(x)$  is the leading twist LCDA of the meson  $\phi$ , and the ellipsis denotes additional parts that have no contributions in our case. It is easy to find that neither Fig. 2(a) nor (b) contributes to the longitudinal polarization amplitude, and the final decay amplitude can be written as

$$\begin{aligned} \mathcal{A}_{\bar{B}^0 \rightarrow \phi \bar{K}^{*0}}^{\text{NP}} &= \frac{G_F}{\sqrt{2}} |V_{ts}| e^{i\delta_T} g'_T (-4i f_\phi^T) \left\{ i \epsilon_{\mu\nu\rho\sigma} \varepsilon_{1\perp}^{*\mu} \varepsilon_2^{*\nu} p^\rho p'^\sigma 2T_1^{B \rightarrow K^*}(m_\phi^2) \right. \\ &+ T_2^{B \rightarrow K^*}(m_\phi^2) \left[ (\varepsilon_{1\perp}^* \cdot \varepsilon_2^*) (m_B^2 - m_{K^*}^2) - 2(\varepsilon_{1\perp}^* \cdot p) (\varepsilon_2^* \cdot p) \right] \\ &\left. - 2T_3^{B \rightarrow K^*}(m_\phi^2) \frac{m_\phi^2}{m_B^2 - m_{K^*}^2} (\varepsilon_{1\perp}^* \cdot p) (\varepsilon_2^* \cdot p) \right\}, \end{aligned} \quad (19)$$

with  $g'_T = (1 + \frac{1}{2N_c}) C_{T1} + (\frac{1}{2} + \frac{1}{N_c}) C_{T8}$ . In the helicity basis, the new decay amplitude Eq. (19)



can be further decomposed into

$$H_{00}^{\text{NP}} = 0, \quad (20)$$

$$H_{\pm\pm}^{\text{NP}} = \frac{G_F}{\sqrt{2}} |V_{ts}| e^{i\delta_T} g'_T (4i f_\phi^T) \left[ (m_{B_d}^2 - m_{K^{*0}}^2) T_2^{B \rightarrow K^*}(m_\phi^2) \mp 2m_{B_d} p_c T_1^{B \rightarrow K^*}(m_\phi^2) \right], \quad (21)$$

where  $p_c$  is the center-of-mass momentum of final mesons in  $\bar{B}^0$  rest frame. Compared with the SM predictions Eqs. (40) and (41), the new transverse polarization amplitudes  $H_{\pm\pm}^{\text{NP}}$  are enhanced by a factor of  $m_{B_d}/m_\phi$ , while the longitudinal part remains unchanged. It is therefore expected that these new tensor operators might provide a possible resolution to the polarization anomaly observed in  $B \rightarrow \phi K^*$  decays.

### 2.3 The branching ratios and polarization fractions

From the above discussions, the total decay amplitudes are then given as

$$\mathcal{A} = \mathcal{A}^{\text{SM}} + \mathcal{A}^{\text{NP}}, \quad (22)$$

where  $\mathcal{A}^{\text{SM}}$  denotes the SM results obtained using the QCDF, and  $\mathcal{A}^{\text{NP}}$  the contributions of the particular NP scenario with anomalous tensor operators in Eq. (8). The corresponding branching ratios are

$$\mathcal{B}(B^{0,+} \rightarrow \eta K^{(*)0,+}) = \frac{\tau_B p_c}{8\pi m_B^2} |\mathcal{A}(B^{0,+} \rightarrow \eta K^{(*)0,+})|^2, \quad (23)$$

$$\mathcal{B}(\bar{B}^0 \rightarrow \phi \bar{K}^{*0}) = \frac{\tau_B p_c}{8\pi m_B^2} (|H_{00}|^2 + |H_{++}|^2 + |H_{--}|^2), \quad (24)$$

where  $\tau_B$  is the life time of  $B$  meson.

In the transversity basis [39], the decay amplitude for any  $\bar{B} \rightarrow VV$  decay can also be decomposed into another three quantities  $A_0$ ,  $A_\parallel$ , and  $A_\perp$ , which are related to the helicity amplitudes  $H_{00}$ ,  $H_{++}$ , and  $H_{--}$  through

$$A_0 = H_{00}, \quad A_\parallel = \frac{H_{++} + H_{--}}{\sqrt{2}}, \quad A_\perp = -\frac{H_{++} - H_{--}}{\sqrt{2}}. \quad (25)$$

In terms of these quantities, we can express the longitudinal polarization fraction as

$$\begin{aligned} f_L &= \frac{|A_0|^2}{|A_0|^2 + |A_\parallel|^2 + |A_\perp|^2} \\ &= \frac{|H_{00}|^2}{|H_{00}|^2 + |H_{++}|^2 + |H_{--}|^2}. \end{aligned} \quad (26)$$

In addition, the relative phases between these helicity amplitudes  $\phi_{\parallel,\perp} = \text{Arg}(A_{\parallel,\perp}/A_0) + \pi$  (the definition of these observables is compatible with that used by the BABAR and Belle collaborations [11, 12]), are potentially very useful for constraining the parameter spaces of NP scenario, however, depend on whether the strong phases of the helicity amplitudes could be calculated reliably.

### 3 Numerical analysis and discussions

With the theoretical formulas and the input parameters summarized in Appendix B for the decay modes of our concerns, we now go to our numerical analysis and discussions.

As shown by the NP decay amplitudes Eqs. (12)–(15) and (20)–(21), the allowed regions for the parameters  $g_T$  and  $\delta_T$  can be obtained from the four measured  $\mathcal{B}(B^{0,+} \rightarrow \eta K^{(*)0,+})$ , and the ones for  $g'_T$  from  $\mathcal{B}(B^0 \rightarrow \phi K^{*0})$  and  $f_L$ , respectively. Generally, we have five branching ratios and one polarization fraction, but only three free parameters: one NP weak phase  $\delta_T$  and two effective coefficients  $g_T$  and  $g'_T$  (or equivalently  $C_{T1}$  and  $C_{T8}$ ). So, it is easy to guess that these decays could severely constrain or rule out the NP scenario with two anomalous tensor operators Eq. (8).

To make the guess clear, we shall first find out the allowed regions for the parameters  $g_T$  and  $\delta_T$  from the four  $B^{0,+} \rightarrow \eta K^{(*)0,+}$  decays. Then, using the allowed regions for the weak phase  $\delta_T$ , we try to put constraint on the parameter  $g'_T$  from  $\mathcal{B}(B^0 \rightarrow \phi K^{*0})$  and  $f_L$ . Finally, we can obtain the allowed parameter spaces, if there are, for  $C_{T1}$ ,  $C_{T8}$ , and  $\delta_T$  that satisfy all the experimental data on the decay modes of our concerns. To further test the particular NP scenario Eq. (8), we also present our theoretical predictions for  $B_s \rightarrow \phi\phi$  decay. Theoretical estimations of the annihilation contributions at present suffer from very large uncertainties, which of course will dilute the requirement of NP very much. To show the dilution, we will give our numerical results for two cases, i.e., with and without annihilations for comparison.

#### 3.1 Constraints on the NP parameters from $B^{0,+} \rightarrow \eta K^{(*)0,+}$ decays

Since the tensor operator contributions to the decay amplitudes of the four  $B^{0,+} \rightarrow \eta K^{(*)0,+}$  decays are all characterized by the parameters  $g_T$  and  $\delta_T$ , possible regions for these two NP

parameters can be obtained from the measured branching ratios of  $B^{0,+} \rightarrow \eta K^{(*)0,+}$  decays. Our main results are shown in Tables 1–2 and Figs. 3–4. The experimental data listed in Table 1 are taken from the Heavy Flavor Averaging Group (HFAG) [2]. The SM predictions for the branching ratios of these four decays are presented in the third column of Table 1, where the theoretical uncertainties are obtained by varying the input parameters within the regions specified in Eq. (7) and Appendix B. For each decay mode, the first and the second row are evaluated with and without the annihilation contributions, respectively.

Table 1: Experimental data [2] and theoretical predictions for the branching ratios (in units of  $10^{-6}$ ). The numbers in columns Case I and Case II are our fitting results with  $g_T$  and  $\delta_T$  constrained by varying the experimental data within  $1\sigma$  and  $2\sigma$  error bars, respectively. For each decay mode, the first (second) row is evaluated with(out) the annihilation contributions.

Decay channel	Experiment	SM	Case I	Case II
$B^- \rightarrow \eta K^-$	$2.2 \pm 0.3$	$2.21^{+1.35}_{-0.85}$	$2.29^{+0.12}_{-0.18}$	$2.19^{+0.35}_{-0.33}$
		$1.80 \pm 0.82$	$2.19 \pm 0.27$	$2.17 \pm 0.34$
$B^0 \rightarrow \eta K^0$	$< 1.9$	$1.34^{+1.09}_{-0.65}$	$1.30^{+0.14}_{-0.14}$	$1.25^{+0.31}_{-0.28}$
		$1.02 \pm 0.65$	$1.42 \pm 0.22$	$1.34 \pm 0.30$
$B^- \rightarrow \eta K^{*-}$	$19.5^{+1.6}_{-1.5}$	$6.27^{+3.4}_{-2.3}$	$18.15^{+0.21}_{-0.09}$	$17.44^{+0.68}_{-0.55}$
		$5.03 \pm 1.82$	$17.88 \pm 0.49$	$17.45 \pm 0.61$
$B^0 \rightarrow \eta K^{*0}$	$16.1 \pm 1.0$	$6.87^{+3.5}_{-2.5}$	$16.96^{+0.09}_{-0.16}$	$17.13^{+0.56}_{-0.68}$
		$5.60 \pm 1.95$	$17.10 \pm 0.29$	$17.03 \pm 0.65$

From Table 1, we can see that the theoretical predictions within the SM for both  $\mathcal{B}(B^- \rightarrow \eta K^-)$  and  $\mathcal{B}(B^0 \rightarrow \eta K^0)$  agree with the experimental data within errors. However, both  $\mathcal{B}(B^- \rightarrow \eta K^{*-})$  and  $\mathcal{B}(B^0 \rightarrow \eta K^{*0})$  are quite lower than the experimental data. We also note that our results are a little different with those in Refs. [8, 9, 23], due to different choices for the input parameters, such as the moderate strength of  $X_A$ ,  $\lambda_B$ , and so on.

As shown in Fig. 3, the four  $\mathcal{B}(B^{0,+} \rightarrow \eta K^{(*)0,+})$  are very sensitive to the presence of the  $\mathcal{H}_{eff}^{NP}$  of Eq. (8). The two bands for the parameter spaces constrained by  $B^- \rightarrow \eta K^-$  and  $B^0 \rightarrow \eta K^0$  decays are much overlapped, and the same situation is also found for the two bands

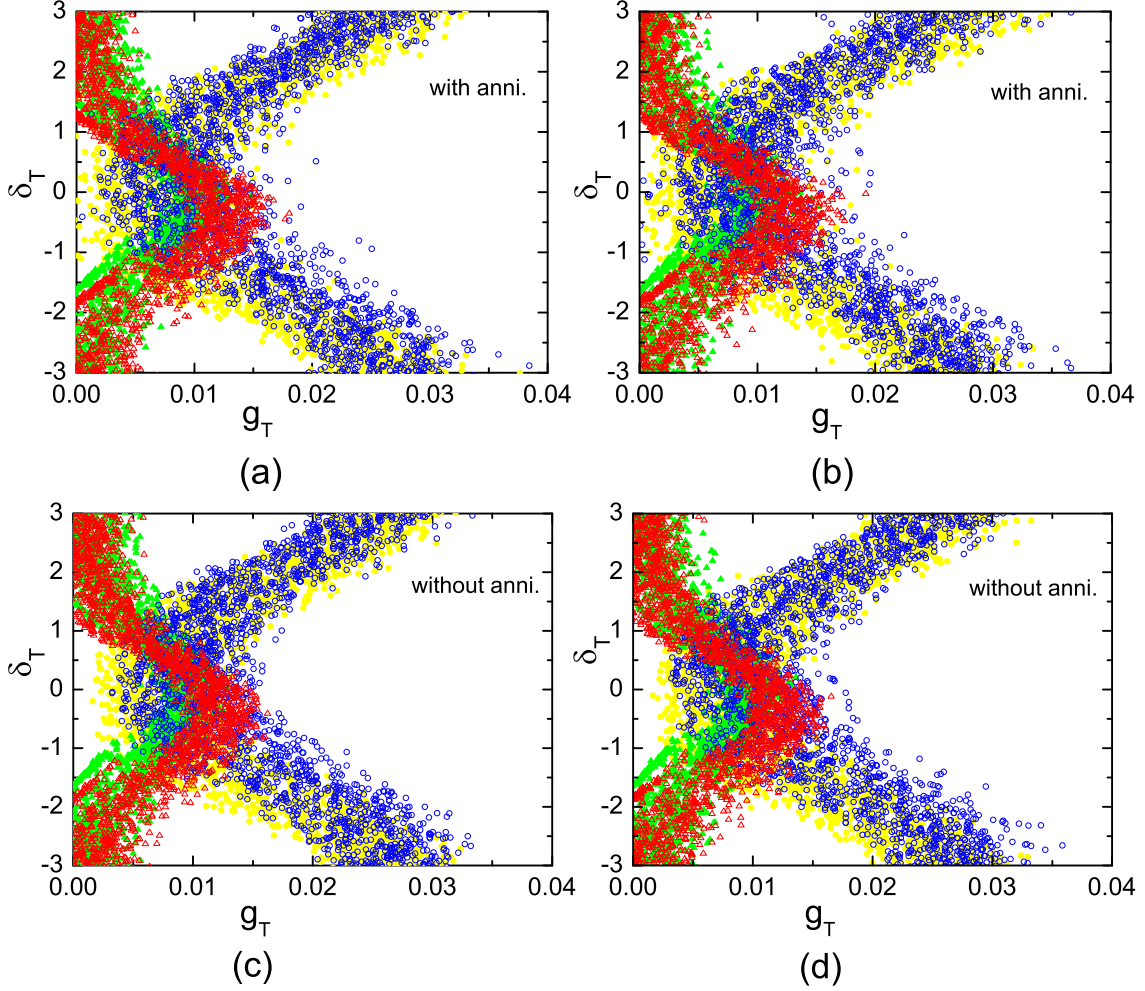


Figure 3: The contour plots for the parameters  $g_T$  and  $\delta_T$  with the experimental data varying within  $1\sigma$  ((a) and (c)) and  $2\sigma$  ((b) and (d)) error bars, respectively. The red triangle, green triangle, blue circle, and yellow circle bands come from the decays  $B^- \rightarrow \eta K^-$ ,  $B^0 \rightarrow \eta K^0$ ,  $B^- \rightarrow \eta K^{*-}$ , and  $B^0 \rightarrow \eta K^{*0}$ , respectively. Plots labels ‘with(out) anni.’ denote the results with(out) the annihilation contributions.

constrained by  $B^- \rightarrow \eta K^{*-}$  and  $B^0 \rightarrow \eta K^{*0}$  decays. However, we note that  $\mathcal{B}(B \rightarrow \eta K)$  and  $\mathcal{B}(B \rightarrow \eta K^*)$  have quite different dependence on these NP contributions. So, the allowed regions for the parameters  $g_T$  and  $\delta_T$  are severely narrowed down when constraints from these four decay modes are combined.

The final allowed regions for the parameters  $g_T$  and  $\delta_T$  extracted from the four  $B^{0,+} \rightarrow \eta K^{(*)0,+}$  decays are shown in Fig. 4, where the left (right) plot is the results with(out) the annihilation contributions. In addition, the dark and the gray regions in Fig. 4 correspond to

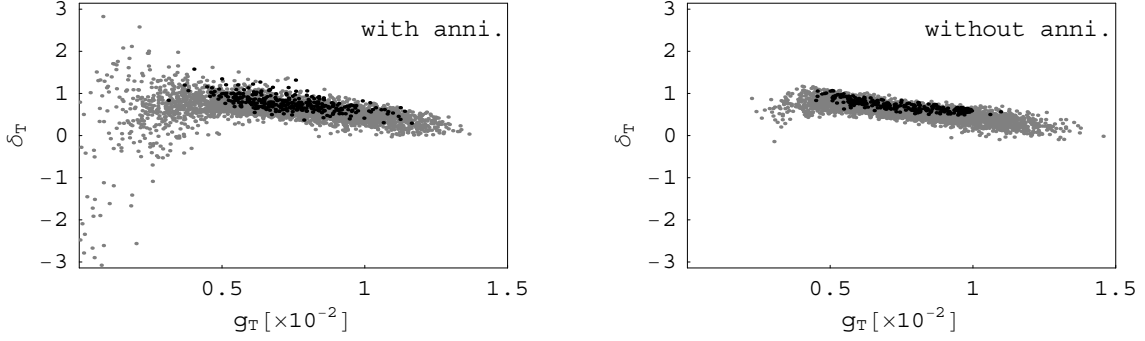


Figure 4: The allowed regions for the parameters  $g_T$  and  $\delta_T$  constrained by the four  $B^{0,+} \rightarrow \eta K^{(*)0,+}$  decays. The dark and the gray regions correspond to the results obtained with the measured branching ratios varying within  $1\sigma$  and  $2\sigma$  error bars, respectively. The left (right) plot denotes the results with(out) the annihilation contributions.

the results obtained with the measured branching ratios varying within  $1\sigma$  and  $2\sigma$  error bars, respectively. From now on, we denote these two possible regions by Case I and Case II. Comparing the two plots in Fig. 4, one can find that the uncertainties of annihilation contributions would loosen constraints on the NP parameters, especially on  $\delta_T$ . The numerical results for the parameters  $g_T$  and  $\delta_T$  corresponding to the above two allowed regions are presented in Table 2.

As shown in Table 1, with the parameters  $g_T$  and  $\delta_T$  varying within these two allowed regions, the large  $\mathcal{B}(B^- \rightarrow \eta K^{*-})$  and  $\mathcal{B}(B^0 \rightarrow \eta K^{*0})$  can be accounted for by the anomalous four-quark tensor operators without violating  $\mathcal{B}(B^- \rightarrow \eta K^-)$ . It is also interesting to note that, taking the 90% CL upper limit of  $\mathcal{B}(B^0 \rightarrow \eta K^0)$  as an input, our fitting result for  $\mathcal{B}(B^0 \rightarrow \eta K^0)$  is in good agreement with the very recent measurements

$$\mathcal{B}(B^0 \rightarrow \eta K^0) = (1.8_{-0.6}^{+0.7} \pm 0.1) \times 10^{-6} \quad \text{BABAR [5]}, \quad (27)$$

$$\mathcal{B}(B^0 \rightarrow \eta K^0) = (1.1 \pm 0.4 \pm 0.1) \times 10^{-6} \quad \text{Belle [6]}, \quad (28)$$

which give the average value  $\mathcal{B}(B^0 \rightarrow \eta K^0) = (1.3 \pm 0.3) \times 10^{-6}$ .

### 3.2 Constraints on the NP parameters from $B^0 \rightarrow \phi K^{*0}$ decay

Now we discuss constraints on the NP parameters from  $B^0 \rightarrow \phi K^{*0}$  decay. With the NP weak phase  $\delta_T$  already extracted from the four  $B^{0,+} \rightarrow \eta K^{(*)0,+}$  decays, the parameter  $g'_T$  could be severely constrained by the well measured  $\mathcal{B}(B^0 \rightarrow \phi K^{*0})$  and  $f_L$ . Our results are presented in

Table 2: The numerical results for the parameters  $g_T$  and  $\delta_T$ , corresponding to the two allowed regions shown in Fig. 4. The allowed regions for the parameter  $g'_T$  constrained by  $B^0 \rightarrow \phi K^{*0}$  decay are also presented. For each case, the first (second) row denotes the results with(out) the annihilation contributions.

	Allowed region	$g_T(\times 10^{-3})$	$g'_T(\times 10^{-3})$	$\delta_T(\text{rad})$
Case I	dark	$7.3^{+1.6}_{-1.5}$	$7.6^{+1.0}_{-0.9}$	$0.77^{+0.20}_{-0.16}$
		$7.7 \pm 1.6$	$8.9 \pm 0.5$	$0.70 \pm 0.13$
Case II	gray	$7.2^{+2.5}_{-2.8}$	$8.3^{+1.3}_{-1.2}$	$0.60^{+0.29}_{-0.39}$
		$8.0 \pm 2.3$	$9.1 \pm 0.6$	$0.55 \pm 0.20$

Table 3: Experimental data [2] and theoretical predictions for the observables in  $B^0 \rightarrow \phi K^{*0}$  decay. The other captions are the same as in Table 1.

Observable	Experiment	SM	Case I	Case II
$\mathcal{B}(\times 10^{-6})$	$9.5 \pm 0.9$	$5.9^{+1.2}_{-1.0}$	$9.6^{+0.5}_{-0.6}$	$9.9^{+0.8}_{-1.1}$
		$5.7 \pm 0.6$	$10.0 \pm 0.3$	$10.3 \pm 0.7$
$f_L$	$0.49 \pm 0.04$	$0.76^{+0.06}_{-0.07}$	$0.50^{+0.02}_{-0.02}$	$0.54^{+0.02}_{-0.03}$
		$0.78 \pm 0.03$	$0.52 \pm 0.01$	$0.55 \pm 0.01$
$\phi_{\parallel}(\text{rad})$	$2.41^{+0.18}_{-0.16}$	$2.90^{+0.25}_{-0.27}$	$1.95^{+0.13}_{-0.12}$	$1.81^{+0.34}_{-0.18}$
		$2.91 \pm 0.01$	$1.82 \pm 0.05$	$1.72 \pm 0.08$
$\phi_{\perp}(\text{rad})$	$2.52 \pm 0.17$	$2.90^{+0.25}_{-0.27}$	$1.96^{+0.13}_{-0.12}$	$1.83^{+0.38}_{-0.18}$
		$2.91 \pm 0.01$	$1.82 \pm 0.05$	$1.73 \pm 0.08$

Table 3, Figs. 5 and 6.

From Table 3, we can see that, with our choice for the input parameters, especially our quite optimistic choice for the annihilation contributions, the SM predictions for both  $\mathcal{B}(B^0 \rightarrow \phi K^{*0})$  and  $f_L$  deviate from the experimental data, and possible NP scenarios beyond the SM may be needed to resolve the observed polarization anomaly.

Fig. 5 shows the dependence of  $\mathcal{B}(B^0 \rightarrow \phi K^{*0})$  and  $f_L$  on the parameter  $g'_T$ , with the NP

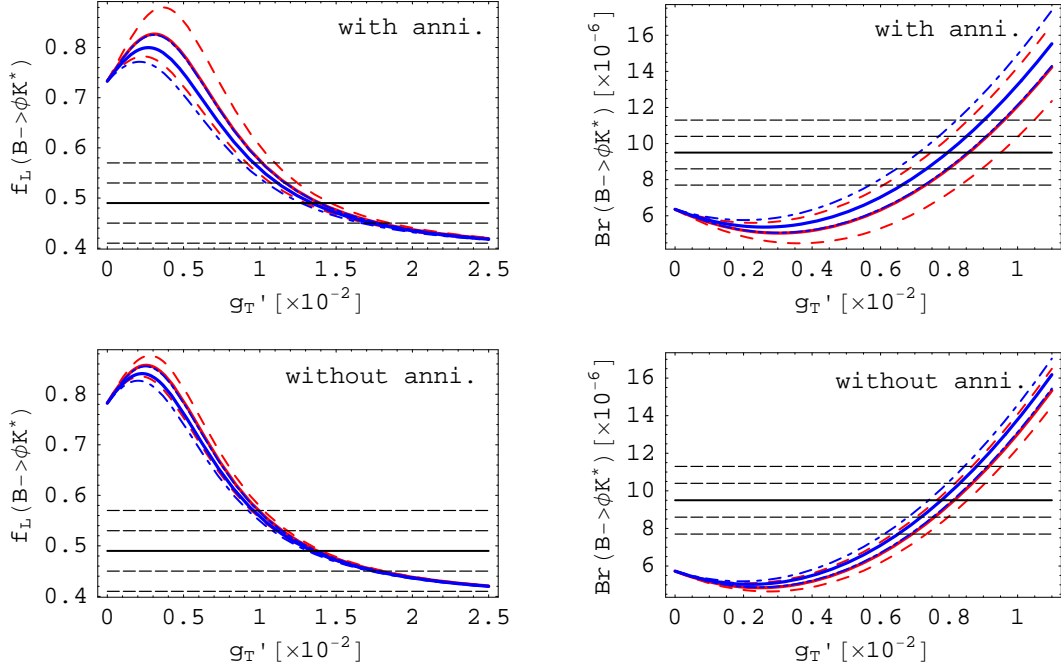


Figure 5: The dependence of  $\mathcal{B}(B^0 \rightarrow \phi K^{*0})$  and  $f_L(B^0 \rightarrow \phi K^{*0})$  on the parameter  $g'_T$  with the NP weak phase  $\delta_T$  extracted from the four  $B^{0,+} \rightarrow \eta K^{(*)0,+}$  decays. The upper and the lower plots denote the results with and without the annihilation contributions, respectively. In each plots, the solid blue (red) curves are the results with  $\delta_T$  given by Case I (II), and dashed curves due to the error bars of this parameter. The horizontal lines are the experimental data with the solid lines being the central values and the dashed ones the error bars ( $1\sigma$  and  $2\sigma$ ).

weak phase  $\delta_T$  extracted from the four  $B^{0,+} \rightarrow \eta K^{(*)0,+}$  decays. To illuminate the dependence more clearly, we have taken all the other input parameters to be their center values. As shown in Fig. 5, both  $\mathcal{B}(B^0 \rightarrow \phi K^{*0})$  and  $f_L$  are very sensitive to the parameter  $g'_T$ . It is particularly interesting to note that the variation trends of these two observables relative to the parameter  $g'_T$  are opposite to each other. Thus, with the allowed regions for the NP weak phase  $\delta_T$  extracted from the four  $B^{0,+} \rightarrow \eta K^{(*)0,+}$  decays, and the experimental data on these two observables, we could get constraints on the parameter  $g'_T$ . The final allowed regions for the parameters  $g'_T$  and  $\delta_T$  are shown in Fig. 6, with the corresponding numerical results given in Table 2.

Corresponding to the two allowed regions for the parameters  $g'_T$  and  $\delta_T$  given in Table 2, both  $\mathcal{B}(B^0 \rightarrow \phi K^{*0})$  and  $f_L$  are in good agreement with the experimental data as shown in Table 3. On the other hand, without the annihilation contributions, our predictions for the relative phases  $\phi_{\parallel}$  and  $\phi_{\perp}$  in the decay  $B^0 \rightarrow \phi K^{*0}$  are not consistent with the experimental

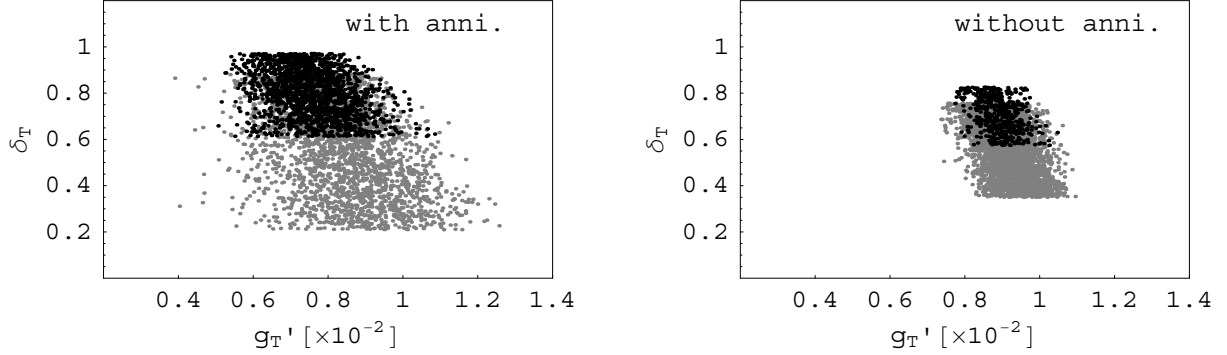


Figure 6: The allowed regions for the parameters  $g_T'$  constrained by  $\mathcal{B}(B^0 \rightarrow \phi K^{*0})$  and  $f_L$  with the NP weak phase  $\delta_T$  extracted from the four  $B^{0,+} \rightarrow \eta K^{(*)0,+}$  decays. Other captions are the same as in Fig. 4.

data. This mismatch is, however, reduced by including the annihilation contributions associated with strong phase, which may indicate the annihilation contributions to be complex. We also note that the annihilation contributions have been proved recently to be real and power suppressed [40]. Moreover, in Ref. [41], it is found that the NP strong phases are generally negligibly small compared to those of the SM contributions. Further discussion of possible resolution to the mismatch would be beyond the scope of this paper.

### 3.3 Final allowed regions for NP parameters and predictions for $B_s \rightarrow \phi\phi$ decay

Finally, using the relations

$$g_T = C_{T8} + \frac{C_{T1}}{N_c}, \quad (29)$$

$$g_T' = \left(1 + \frac{1}{2N_c}\right) C_{T1} + \left(\frac{1}{2} + \frac{1}{N_c}\right) C_{T8}, \quad (30)$$

with  $N_c = 3$ , we get the final allowed regions for the parameters  $C_{T1}$  and  $C_{T8}$ , which are presented in Table 4. It is interesting to note that the color-octet operator  $O_{T8}$  dominates the NP contributions. Actually, with  $O_{T8}$  only, we obtain  $C_{T8} = (7.3^{+1.6}_{-1.5}) \times 10^{-3}$   $((7.7 \pm 1.6) \times 10^{-3})$  and  $C_{T8} = (9.1^{+1.2}_{-1.0}) \times 10^{-3}$   $((10.7 \pm 0.6) \times 10^{-3})$  from  $B \rightarrow \eta K^{(*)}$  and  $B \rightarrow \phi K^*$  decays, respectively, where (also for the following results) the numbers in the bracket are obtained without the annihilation contributions. Thus, we obtain a single color-octet  $O_{T8}$  solution with



Table 4: Final results for the coefficients  $C_{T1}$ ,  $C_{T8}$ , and the weak phase  $\delta_T$  extracted from  $B \rightarrow \eta K^{(*)}$  and  $B^0 \rightarrow \phi K^{*0}$  decays. The other captions are the same as in Table 2.

Allowed region		$C_{T1}(\times 10^{-3})$	$C_{T8}(\times 10^{-3})$	$\delta_T(\text{rad})$
Case I	dark	$1.7^{+1.9}_{-1.7}$	$6.8^{+2.2}_{-1.9}$	$0.77^{+0.20}_{-0.16}$
		$2.8 \pm 1.6$	$6.7 \pm 2.1$	$0.70 \pm 0.13$
Case II	gray	$2.6^{+2.8}_{-3.0}$	$6.4^{+3.3}_{-3.7}$	$0.60^{+0.29}_{-0.39}$
		$2.8 \pm 2.2$	$7.1 \pm 3.0$	$0.55 \pm 0.20$

$C_{T8} = (8.5^{+0.9}_{-0.9}) \times 10^{-3}$  ( $(10.3 \pm 0.5) \times 10^{-3}$ ) and  $\delta_T = 44.1^{+11.6^\circ}_{-9.0^\circ}$  ( $40.2^\circ \pm 7.2^\circ$ ). However, with the color-singlet operator  $O_{T1}$  only, we could not get any solution.

It is noted that the two tensor operators  $O_{T1}$  and  $O_{T8}$  could be expressed by the other two (pseudo-) scalar operators  $O_{S+P}$  and  $O'_{S+P}$  through the Fierz transformation relations [18]

$$O_{S+P} = \frac{1}{12}O_{T1} - \frac{1}{6}O_{T8}, \quad O'_{S+P} = \frac{1}{12}O_{T8} - \frac{1}{6}O_{T1}. \quad (31)$$

Such operators could be generated in many NP scenarios with scalar interactions. It would be useful to present the constraints on the coefficients of the two  $(S+P) \otimes (S+P)$  operators. To this end, we get

$$C_{S+P} = (-0.99^{+0.39}_{-0.35}) \times 10^{-3} \quad ((-0.89 \pm 0.38) \times 10^{-3}), \quad (32)$$

$$C'_{S+P} = (0.29^{+0.36}_{-0.32}) \times 10^{-3} \quad ((0.09 \pm 0.32) \times 10^{-3}), \quad (33)$$

with the normalization factor  $\frac{G_F}{\sqrt{2}}|V_{ts}|$  and a new weak phase  $\delta_T = 44.1^{+11.6^\circ}_{-9.0^\circ}$  ( $40.2^\circ \pm 7.2^\circ$ ), corresponding to the two tensor operators case. The single  $O_{T8}$  solution would correspond to  $C_{S+P} \equiv -2C'_{S+P} = (-1.4^{+0.1}_{-0.2}) \times 10^{-3}$  ( $(-1.7 \pm 0.1) \times 10^{-3}$ ), and the weak phase is the same as the former. It should be noted that the relation  $C_{S+P} = -2C'_{S+P}$  is strictly required for the last correspondence.

To further test the particular NP scenario with anomalous tensor operators Eq. (8), we also present our theoretical predictions for the branching ratio and the longitudinal polarization fraction of  $B_s \rightarrow \phi\phi$  decay, as summarized in Table 5. Within the SM, its decay amplitude is

Table 5: Theoretical predictions for  $B_s \rightarrow \phi\phi$  decay both within the SM and in the particular NP scenario Eq. (8). The other captions are the same as in Table 1.

Observable	Experiment	SM	Case I	Case II
$\mathcal{B}(\times 10^{-6})$	$14^{+8}_{-7}$	$20.6^{+4.2}_{-3.0}$	$29.4^{+4.4}_{-3.5}$	$20.1^{+5.9}_{-4.8}$
		$17 \pm 2$	$30 \pm 3$	$29 \pm 3$
$f_L$	—	$0.83^{+0.04}_{-0.06}$	$0.73^{+0.07}_{-0.08}$	$0.72^{+0.07}_{-0.07}$
		$0.83 \pm 0.02$	$0.66 \pm 0.03$	$0.67 \pm 0.03$

given by [15]

$$\begin{aligned}
\frac{1}{2}A_{\overline{B}_s \rightarrow \phi\phi}^{\text{SM}} = & A_{\phi\phi} \sum_{p=u,c} V_{pb}V_{ps}^* \left[ \alpha_3^{p,h} + \alpha_4^{p,h} - \frac{1}{2}\alpha_{3,\text{EW}}^{p,h} - \frac{1}{2}\alpha_{4,\text{EW}}^{p,h} + \beta_3^{p,h} - \frac{1}{2}\beta_{3,\text{EW}}^{p,h} \right. \\
& \left. + \beta_4^{p,h} - \frac{1}{2}\beta_{4,\text{EW}}^{p,h} \right]. \quad (34)
\end{aligned}$$

With respect to the relevant quantities in Eq. (34), one can get them directly from those for  $B^0 \rightarrow \phi K^{*0}$  decay with some simple changes. This decay mode is of particular interest to test the proposed resolutions to the polarization anomalies observed in  $B \rightarrow \phi K^*$  decays, since both of these decay modes are mediated by the same quark level subprocess  $b \rightarrow s\bar{s}s$ . In addition, since the two final-state mesons are identical in this decay mode, more observables in the time-dependent angular analysis will become zero [39]. So, this decay mode can be considered as an ideal probe for various NP scenarios proposed to resolve the polarization anomalies observed in  $B \rightarrow \phi K^*$  decays. The earlier studies of this particular decay mode within the QCDF formalism have been carried out in Ref. [42], but without taking into account the annihilation contributions.

From the numerical results presented in Tables 3 and 5, we can see that both the branching ratio and the longitudinal polarization fraction of  $B_s \rightarrow \phi\phi$  decay is larger than those of the decay  $B^0 \rightarrow \phi K^{*0}$ , which is due to the relative factor of two in the  $\phi\phi$  amplitude Eq. (34), as well as the additional contribution from the annihilation coefficient  $\beta_4^{p,h}$ . In particular, due to an accidental cancelation, the annihilation coefficient  $\beta_3^{p,0}$  (contributing to both  $H_{00}(B^0 \rightarrow \phi K^{*0})$  and  $H_{00}(B_s \rightarrow \phi\phi)$ ) is quite smaller than  $\beta_4^{p,0}$  [15]. Interestingly, recent calculations made in the perturbative QCD approach also predict a large branching

ratio  $\mathcal{B}(B_s \rightarrow \phi\phi) = (44.1_{-6.5}^{+8.3+13.3+0.0}) \times 10^{-6}$  with the longitudinal polarization fraction  $f_L(B_s \rightarrow \phi\phi) = (68.0_{-4.0-2.2-0.0}^{+4.2+1.7+0.0}) \times 10^{-2}$  [43]. Their result for  $f_L(B_s \rightarrow \phi\phi)$  is smaller than our predictions within the SM. The predicted results presented in Table 5 could be tested at the Fermilab Tevatron and the LHC-b experiments.

## 4 Conclusions

In summary, motivated by the observed discrepancies between the experimental data and the SM predictions for the branching ratios of  $B \rightarrow \eta K^*$  decays and the polarization fractions in  $B \rightarrow \phi K^*$  decays, we have studied a particular NP scenario with anomalous tensor operators  $O_{T1}$  and  $O_{T8}$ , which has been proposed to resolve the polarization anomalies in the literature [17, 18, 19].

After extensive numerical analysis, we have found that the above observed discrepancies could be resolved simultaneously and constraints on the NP parameters have been obtained. With both the experimental data and the theoretical input parameters varying within  $1\sigma$  error bars, we have found the following two solutions: (I) both the two tensor operators contribute with the parameter spaces presented in the upper two rows of Table 4; (II) only  $O_{T8}$  contributes with  $C_{T8} = (8.5_{-0.9}^{+0.9}) \times 10^{-3} ((10.3 \pm 0.5) \times 10^{-3})$  and  $\delta_T$  the same as solution (I). The above two solutions correspond to the scenario with new operators  $O_{S+P}$  and  $O'_{S+P}$  added to the SM, with the parameter spaces: (I)  $C_{S+P} = (-0.99_{-0.35}^{+0.39}) \times 10^{-3} ((-0.89 \pm 0.38) \times 10^{-3})$ ,  $C''_{S+P} = (0.29_{-0.32}^{+0.36}) \times 10^{-3} ((0.09 \pm 0.32) \times 10^{-3})$  and (II)  $C_{S+P} \equiv -2C''_{S+P} = (-1.4_{-0.2}^{+0.1}) \times 10^{-3} ((-1.7 \pm 0.1) \times 10^{-3})$ . Their weak phase  $\delta_{S+P}$  is the same as  $\delta_T$ .

Against our early expectations, we have found that the solution with two tensor operators are dominated by the color-octet operator  $O_{T8}$ . It would be interesting to investigate whether the available NP models could give such effective interactions at the  $m_b$  scale.

To further test the particular NP scenario with two anomalous tensor operators  $O_{T1,T8}$  or (pseudo-) scalar operators  $O_{S+P}^{(\prime)}$ , we have also presented our predictions for the observables in  $B_s \rightarrow \phi\phi$  decay, which could be tested more thoroughly at the Fermilab Tevatron and the LHC-b experiments in the near future.

It should be noted that the strong constraints in Table 4 obtained without annihilation

contributions may be too optimistic. As has been shown in the table, the uncertainties due to poorly known annihilation contributions could dilute the requirement of NP very much. Generally, this caveat could be applied to probe possible NP scenarios in exclusive non-leptonic  $B$  decays. Further theoretical progress is strongly demanded.

## Acknowledgments

The work is supported by National Science Foundation under contract Nos. 10305003 and 10675039, and the NCET Program sponsored by Ministry of Education, China.

## Appendix A: Decay amplitudes in the SM with QCDF

The amplitudes for  $B \rightarrow \eta K^{(*)}$  are recapitulated from Ref. [23]

$$\begin{aligned} \sqrt{2} \mathcal{A}_{B^- \rightarrow K^- \eta}^{\text{SM}} = & \sum_{p=u,c} V_{pb} V_{ps}^* \left\{ A_{K^- \eta q} \left[ \delta_{pu} \alpha_2 + 2\alpha_3^p + \frac{1}{2} \alpha_{3,\text{EW}}^p \right] \right. \\ & + \sqrt{2} A_{K^- \eta s} \left[ \delta_{pu} \beta_2 + \alpha_3^p + \alpha_4^p - \frac{1}{2} \alpha_{3,\text{EW}}^p - \frac{1}{2} \alpha_{4,\text{EW}}^p + \beta_3^p + \beta_{3,\text{EW}}^p \right] \\ & \left. + A_{\eta q K^-} \left[ \delta_{pu} (\alpha_1 + \beta_2) + \alpha_4^p + \alpha_{4,\text{EW}}^p + \beta_3^p + \beta_{3,\text{EW}}^p \right] \right\}, \end{aligned} \quad (35)$$

$$\begin{aligned} \sqrt{2} \mathcal{A}_{B^0 \rightarrow \bar{K}^0 \eta}^{\text{SM}} = & \sum_{p=u,c} V_{pb} V_{ps}^* \left\{ A_{\bar{K}^0 \eta q} \left[ \delta_{pu} \alpha_2 + 2\alpha_3^p + \frac{1}{2} \alpha_{3,\text{EW}}^p \right] \right. \\ & + \sqrt{2} A_{\bar{K}^0 \eta s} \left[ \alpha_3^p + \alpha_4^p - \frac{1}{2} \alpha_{3,\text{EW}}^p - \frac{1}{2} \alpha_{4,\text{EW}}^p + \beta_3^p - \frac{1}{2} \beta_{3,\text{EW}}^p \right] \\ & \left. + A_{\eta q \bar{K}^0} \left[ \alpha_4^p - \frac{1}{2} \alpha_{4,\text{EW}}^p + \beta_3^p - \frac{1}{2} \beta_{3,\text{EW}}^p \right] \right\}, \end{aligned} \quad (36)$$

$$\begin{aligned} \sqrt{2} \mathcal{A}_{B^- \rightarrow K^{*-} \eta}^{\text{SM}} = & \sum_{p=u,c} V_{pb} V_{ps}^* \left\{ A_{K^{*-} \eta q} \left[ \delta_{pu} \alpha_2 + 2\alpha_3^p + \frac{1}{2} \alpha_{3,\text{EW}}^p \right] \right. \\ & + \sqrt{2} A_{K^{*-} \eta s} \left[ \delta_{pu} \beta_2 + \alpha_3^p + \alpha_4^p - \frac{1}{2} \alpha_{3,\text{EW}}^p - \frac{1}{2} \alpha_{4,\text{EW}}^p + \beta_3^p + \beta_{3,\text{EW}}^p \right] \\ & \left. + A_{\eta q K^{*-}} \left[ \delta_{pu} (\alpha_1 + \beta_2) + \alpha_4^p + \alpha_{4,\text{EW}}^p + \beta_3^p + \beta_{3,\text{EW}}^p \right] \right\}, \end{aligned} \quad (37)$$

$$\begin{aligned}
\sqrt{2} \mathcal{A}_{\overline{B}^0 \rightarrow \overline{K}^{*0} \eta}^{\text{SM}} &= \sum_{p=u,c} V_{pb} V_{ps}^* \left\{ A_{\overline{K}^{*0} \eta_q} \left[ \delta_{pu} \alpha_2 + 2\alpha_3^p + \frac{1}{2} \alpha_{3,\text{EW}}^p \right] \right. \\
&\quad + \sqrt{2} A_{\overline{K}^{*0} \eta_s} \left[ \alpha_3^p + \alpha_4^p - \frac{1}{2} \alpha_{3,\text{EW}}^p - \frac{1}{2} \alpha_{4,\text{EW}}^p + \beta_3^p - \frac{1}{2} \beta_{3,\text{EW}}^p \right] \\
&\quad \left. + A_{\eta_q \overline{K}^{*0}} \left[ \alpha_4^p - \frac{1}{2} \alpha_{4,\text{EW}}^p + \beta_3^p - \frac{1}{2} \beta_{3,\text{EW}}^p \right] \right\}, \tag{38}
\end{aligned}$$

where the explicit expressions for the coefficients  $\alpha_i^p \equiv \alpha_i^p(M_1 M_2)$  and  $\beta_i^p \equiv \beta_i^p(M_1 M_2)$  could also be found in Ref. [23]. We recall that the  $\alpha_i^p$  terms contain one-loop vertex, penguin and hard spectator contributions, whereas the  $\beta_i^p$  terms are due to the weak annihilation, and the transition form factors are encoded in the factors  $A_{M_1 M_2}$ .

The decay amplitude of  $\overline{B}^0 \rightarrow \phi \overline{K}^{*0}$  mode can be read off from Refs. [15, 16]

$$\mathcal{A}_{\overline{B}^0 \rightarrow \phi \overline{K}^{*0}}^{\text{SM}} = A_{\overline{K}^{*0} \phi}^h \sum_{p=u,c} V_{pb} V_{ps}^* \left[ \alpha_3^{p,h} + \alpha_4^{p,h} - \frac{1}{2} \alpha_{3,\text{EW}}^{p,h} - \frac{1}{2} \alpha_{4,\text{EW}}^{p,h} + \beta_3^{p,h} - \frac{1}{2} \beta_{3,\text{EW}}^{p,h} \right], \tag{39}$$

where the superscript ‘ $h$ ’ denotes the helicity of two final-state vector mesons, with  $h = 0, +, -$  corresponding to two outgoing longitudinal, positive, and negative helicity vector mesons, respectively.

In the helicity basis, the decay amplitude Eq. (39) can be further decomposed into the following three helicity amplitudes

$$H_{00}^{\text{SM}} = A_{\overline{K}^{*0} \phi}^0 \sum_{p=u,c} V_{pb} V_{ps}^* \left[ \alpha_3^{p,0} + \alpha_4^{p,0} - \frac{1}{2} \alpha_{3,\text{EW}}^{p,0} - \frac{1}{2} \alpha_{4,\text{EW}}^{p,0} + \beta_3^{p,0} - \frac{1}{2} \beta_{3,\text{EW}}^{p,0} \right], \tag{40}$$

$$H_{\pm\pm}^{\text{SM}} = A_{\overline{K}^{*0} \phi}^{\pm} \sum_{p=u,c} V_{pb} V_{ps}^* \left[ \alpha_3^{p,\pm} + \alpha_4^{p,\pm} - \frac{1}{2} \alpha_{3,\text{EW}}^{p,\pm} - \frac{1}{2} \alpha_{4,\text{EW}}^{p,\pm} + \beta_3^{p,\pm} - \frac{1}{2} \beta_{3,\text{EW}}^{p,\pm} \right], \tag{41}$$

with [15]

$$A_{\overline{K}^{*0} \phi}^h \equiv \frac{G_F}{\sqrt{2}} \langle \overline{K}^{*0} | (\bar{s}b)_{V-A} | \overline{B}^0 \rangle \langle \phi | (\bar{s}s)_V | 0 \rangle, \tag{42}$$

$$A_{\overline{K}^{*0} \phi}^0 = \frac{iG_F}{\sqrt{2}} \frac{m_{B_d}^3 f_\phi}{2m_{K^{*0}}} \left[ \left(1 + \frac{m_{K^{*0}}}{m_{B_d}}\right) A_1^{B \rightarrow K^*}(m_\phi^2) - \left(1 - \frac{m_{K^{*0}}}{m_{B_d}}\right) A_2^{B \rightarrow K^*}(m_\phi^2) \right], \tag{43}$$

$$A_{\overline{K}^{*0} \phi}^{\pm} = \frac{iG_F}{\sqrt{2}} m_{B_d} m_\phi f_\phi \left[ \left(1 + \frac{m_{K^{*0}}}{m_{B_d}}\right) A_1^{B \rightarrow K^*}(m_\phi^2) \mp \left(1 - \frac{m_{K^{*0}}}{m_{B_d}}\right) V^{B \rightarrow K^*}(m_\phi^2) \right]. \tag{44}$$

## Appendix B: Theoretical input parameters

### B1. Wilson coefficients and CKM matrix elements

The Wilson coefficients  $C_i(\mu)$  have been evaluated reliably to next-to-leading logarithmic order [24, 44]. Their numerical results in the naive dimensional regularization scheme at the scale  $\mu = m_b$  ( $\mu_h = \sqrt{\Lambda_h m_b}$ ) are given by

$$\begin{aligned} C_1 &= 1.077 \ (1.178), \quad C_2 = -0.174 \ (-0.355), \quad C_3 = 0.013 \ (0.027), \\ C_4 &= -0.034 \ (-0.060), \quad C_5 = 0.008 \ (0.011), \quad C_6 = -0.039 \ (-0.081), \\ C_7/\alpha_{e.m.} &= -0.013 \ (-0.034), \quad C_8/\alpha_{e.m.} = 0.047 \ (0.099), \quad C_9/\alpha_{e.m.} = -1.208 \ (-1.338), \\ C_{10}/\alpha_{e.m.} &= 0.229 \ (0.426), \quad C_{7\gamma} = -0.297 \ (-0.360), \quad C_{8g} = -0.143 \ (-0.168). \end{aligned} \quad (45)$$

The values at the scale  $\mu_h$ , with  $m_b = 4.79$  GeV and  $\Lambda_h = 500$  MeV, should be used in the calculation of hard-spectator and weak annihilation contributions.

For the CKM matrix elements, we adopt the Wolfenstein parameterization [45] and choose the four parameters  $A$ ,  $\lambda$ ,  $\rho$ , and  $\eta$  as [46]

$$A = 0.809 \pm 0.014, \quad \lambda = 0.2272 \pm 0.0010, \quad \bar{\rho} = 0.197^{+0.026}_{-0.030}, \quad \bar{\eta} = 0.339^{+0.019}_{-0.018}, \quad (46)$$

with  $\bar{\rho} = \rho(1 - \frac{\lambda^2}{2})$  and  $\bar{\eta} = \eta(1 - \frac{\lambda^2}{2})$ .

### B2. Quark masses and lifetimes

As for the quark mass, there are two different classes appearing in our calculation. One type is the pole quark mass appearing in the evaluation of penguin loop corrections, and denoted by  $m_q$ . In this paper, we take

$$m_u = m_d = m_s = 0, \quad m_c = 1.64 \text{ GeV}, \quad m_b = 4.79 \text{ GeV}. \quad (47)$$

The other one is the current quark mass which appears in the factor  $r_\chi^M$  through the equation of motion for quarks. This type of quark mass is scale dependent and denoted by  $\overline{m}_q$ . Here we take [1]

$$\overline{m}_s(\mu)/\overline{m}_q(\mu) = 25 \sim 30, \quad \overline{m}_s(2 \text{ GeV}) = (95 \pm 25) \text{ MeV}, \quad \overline{m}_b(\overline{m}_b) = 4.20 \text{ GeV}, \quad (48)$$

where  $\overline{m}_q(\mu) = (\overline{m}_u + \overline{m}_d)(\mu)/2$ , and the difference between  $u$  and  $d$  quark is not distinguished.

As for the lifetimes of  $B$  mesons, we take [1]  $\tau_{B_u} = 1.638$  ps,  $\tau_{B_d} = 1.530$  ps, and  $\tau_{B_s} = 1.466$  ps as our default input values.

### B3. The decay constants and form factors

In this paper, we take the decay constants

$$\begin{aligned} f_B &= (216 \pm 22) \text{ MeV} [47], & f_{B_s} &= (259 \pm 32) \text{ MeV} [47], & f_\pi &= (130.7 \pm 0.4) \text{ MeV} [1], \\ f_K &= (159.8 \pm 1.5) \text{ MeV} [1] & f_{K^*} &= (217 \pm 5) \text{ MeV} [48], & f_\phi &= (231 \pm 4) \text{ MeV} [48], \\ f_{K^*}^\perp(1 \text{ GeV}) &= (185 \pm 10) \text{ MeV} [48], & f_\phi^\perp(1 \text{ GeV}) &= (200 \pm 10) \text{ MeV} [48], \end{aligned} \quad (49)$$

and the form factors [48]

$$\begin{aligned} F_0^{B \rightarrow \eta}(0) &= 0.275 \pm 0.036, & F_0^{B \rightarrow K}(0) &= 0.331 \pm 0.041, & A_0^{B \rightarrow K^*}(0) &= 0.374 \pm 0.033, \\ V^{B \rightarrow K^*}(0) &= 0.411 \pm 0.033, & A_1^{B \rightarrow K^*}(0) &= 0.292 \pm 0.028, & A_2^{B \rightarrow K^*}(0) &= 0.259 \pm 0.027, \\ V^{B_s \rightarrow \phi}(0) &= 0.434 \pm 0.035, & A_1^{B_s \rightarrow \phi}(0) &= 0.311 \pm 0.030, & A_2^{B_s \rightarrow \phi}(0) &= 0.234 \pm 0.028, \\ T_1^{B \rightarrow K^*}(0) &= 0.333 \pm 0.028, & T_2^{B \rightarrow K^*}(0) &= 0.333 \pm 0.028, & T_1^{B_s \rightarrow \phi}(0) &= 0.349 \pm 0.033, \\ T_2^{B_s \rightarrow \phi}(0) &= 0.349 \pm 0.033. \end{aligned} \quad (50)$$

For the parameters related to the  $\eta$ - $\eta'$  mixing, we choose [28]

$$f_q = (1.07 \pm 0.02) f_\pi, \quad f_s = (1.34 \pm 0.06) f_\pi, \quad \phi = 39.3^\circ \pm 1.0^\circ. \quad (51)$$

The other parameters relevant to the meson  $\eta$  can be obtained from the above three ones [9].

### B4. The LCDAs of mesons.

For the LCDAs of mesons, we use their asymptotic forms [36, 38]

$$\begin{aligned} \Phi_P(x) &= \Phi_{\parallel, \perp}^V(x) = g_\perp^{(a)V}(x) = 6x(1-x), & \Phi_p(x) &= 1, \\ \Phi_v(x) &= 3(2x-1), & g_\perp^{(v)V}(x) &= \frac{3}{4} [1 + (2x-1)^2]. \end{aligned} \quad (52)$$

As for the  $B$  meson wave functions, we need only consider the first inverse moment of the leading LCDA  $\Phi_1^B(\xi)$  defined by [22]

$$\int_0^1 \frac{d\xi}{\xi} \Phi_1^B(\xi) \equiv \frac{m_B}{\lambda_B}, \quad (53)$$

where  $\lambda_B = (460 \pm 110) \text{ MeV}$  [49] is the hadronic parameter introduced to parameterize this integral.

## References

- [1] W.M. Yao *et al.* (Particle Data Group), J. Phys. G **33** (2006) 1.
- [2] E. Barberio *et al.* (Heavy Flavor Averaging Group), arXiv:hep-ex/0603003; and online update at: <http://www.slac.stanford.edu/xorg/hfag>.
- [3] H. J. Lipkin, arXiv:hep-ph/0608284; S. Khalil, arXiv:hep-ph/0608157; M. Gronau and J. L. Rosner, Phys. Rev. D **74** (2006) 057503; S. Baek, J. High Energy Phys. **0607** (2006) 025; R. Arnowitt *et al.*, Phys. Lett. B **633** (2006) 748; H. N. Li, S. Mishima, and A. I. Sanda, Phys. Rev. D **72** (2005) 114005; X. Q. Li and Y. D. Yang, Phys. Rev. D **72** (2005) 074007; C. S. Kim, S. Oh, and C. Yu, Phys. Rev. D **72** (2005) 074005; S. Khalil, Phys. Rev. D **72** (2005) 035007.
- [4] S. J. Richichi *et al.* (CLEO Collaboration), Phys. Rev. Lett. **85** (2000) 520.
- [5] B. Aubert *et al.* (BABAR Collaboration), Phys. Rev. Lett. **95** (2005) 131803; Phys. Rev. D **74** (2006) 051106.
- [6] K. Abe *et al.* (Belle Collaboration), arXiv:hep-ex/0608033; C. H. Wang *et al.* (Belle Collaboration), arXiv:hep-ex/0608034.
- [7] H. J. Lipkin, Phys. Lett. B **633** (2006) 540; A. R. Williamson and J. Zupan, Phys. Rev. D **74** (2006) 014003; **74** (2006) 03901(E); J. F. Cheng, C. S. Huang, and X. H. Wu, Nucl. Phys. **B701** (2004) 54; B. Dutta *et al.*, Eur. Phys. J. C **37** (2004) 273 ; B. Dutta, C. S. Kim, and S. Oh, Phys. Rev. Lett. **90** (2003) 011801; C. W. Chiang, M. Gronau, and J. L. Rosner, Phys. Rev. D **68** (2003) 074012 ; A. Kundu and T. Mitra, Phys. Rev. D **67** (2003) 116005; E. Kou and A. I. Sanda, Phys. Lett. B **525** (2002) 240; D. S. Du, D. S. Yang, and G. H. Zhu, arXiv:hep-ph/9912201; D. S. Du, C. S. Kim, and Y. D. Yang, Phys. Lett. B **426** (1998) 133 .
- [8] M. Z. Yang and Y. D. Yang, Nucl. Phys. **B609** (2001) 469 .



- [9] M. Beneke and M. Neubert, Nucl. Phys. **B651** (2003) 225 .
- [10] A. Kundu, S. Nandi, and J. P. Saha, Phys. Lett. B **622** (2005) 102.
- [11] B. Aubert *et al.* (BABAR Collaboration), Phys. Rev. Lett. **91** (2003) 171802; **93** (2004) 231804.
- [12] K. F. Chen *et al.* (Belle Collaboration), Phys. Rev. Lett. **94** (2005) 221804.
- [13] P. Bussey (CDF Collaboration), talk given at the ICHEP 2006.
- [14] C. H. Chen and H. Hatanaka, Phys. Rev. D **73** (2006) 075003 ; C. S. Huang *et al.*, Phys. Rev. D **73** (2006) 034026; S. Baek *et al.*, Phys. Rev. D **72** (2005) 094008; Y. D. Yang, R. M. Wang, and G. R. Lu, Phys. Rev. D **72** (2005) 015009 ; H. n. Li and S. Mishima, Phys. Rev. D **71** (2005) 054025; C. H. Chen and C. Q. Geng, Phys. Rev. D **71** (2005) 115004; H. Y. Cheng, C. K. Chua, and A. Soni, Phys. Rev. D **71** (2005) 014030 ; H. N. Li, Phys. Lett. B **622** (2005) 63; P. Colangelo, F. De Fazio, and T. N. Pham, Phys. Lett. B **597** (2004) 291; M. Ladisa *et al.*, Phys. Rev. D **70** (2004) 114025; E. Alvarez *et al.*, Phys. Rev. D **70** (2004) 115014; C. Dariescu *et al.*, Phys. Rev. D **69** (2004) 112003.
- [15] M. Beneke, J. Rohrer, and D. Yang, Phys. Rev. Lett. **96** (2006) 141801.
- [16] M. Beneke, J. Rohrer, and D. Yang, arXiv:hep-ph/0612290.
- [17] A. L. Kagan, Phys. Lett. B **601** (2004) 151.
- [18] P. K. Das and K. C. Yang, Phys. Rev. D **71** (2005) 094002 .
- [19] C. S. Kim and Y. D. Yang, arXiv:hep-ph/0412364.
- [20] S. Nandi and A. Kundu, J. Phys. G **32** (2006) 835 .
- [21] Y. Y. Charng, T. Kurimoto, and H. n. Li, Phys. Rev. D **74** (2006) 074024; C. H. Chen and C. Q. Geng, Phys. Lett. B **645** (2007) 197.
- [22] M. Beneke *et al.*, Phys. Rev. Lett. **83** (1999) 1914; Nucl. Phys. **B591** (2000) 313; **606** (2001) 245.

- [23] M. Beneke and M. Neubert, Nucl. Phys. **B675** (2003) 333.
- [24] G. Buchalla, A. J. Buras, and M. E. Lautenbacher, Rev. Mod. Phys. **68** (1996) 1125.
- [25] N. Cabibbo, Phys. Rev. Lett. **10** (1963) 531; M. Kobayashi and T. Maskawa, Prog. Theor. Phys. **49** (1973) 652.
- [26] X. Q. Li and Y. D. Yang, Phys. Rev. D **73** (2006) 114027.
- [27] T. Feldmann and T. Hurth, J. High Energy Phys. **11** (2004) 037.
- [28] T. Feldmann, P. Kroll, and B. Stech, Phys. Rev. D **58** (1998) 114006; Phys. Lett. B **449** (1999) 339; T. Feldmann, Int. J. Mod. Phys. A **15** (2000) 159.
- [29] R. Escribano and J. M. Frere, J. High Energy Phys. **0506** (2005) 029.
- [30] J. F. Cheng, C. S. Huang, and X. H. Wu, Phys. Lett. B **585** (2004) 287; C. S. Huang *et al.*, in Ref. [14].
- [31] G. Hiller and F. Krüger, Phys. Rev. D **69** (2004) 074020.
- [32] E. Frlez *et al.* (PIBETA Collaboration), Phys. Rev. Lett. **93** (2004) 181804.
- [33] A. A. Poblaguev, Phys. Rev. D **68** (2003) 054020; Phys. Lett. B **238** (1990) 108.
- [34] M. V. Chizhov, Phys. Part. Nucl. Lett. **2** (2005) 193; Mod. Phys. Lett. A **8** (1993) 2753; Phys. Lett. B **381** (1996) 359.
- [35] P. Herczeg, Phys. Rev. D **49** (1994) 247; M. B. Voloshin, Phys. Lett. B **283** (1992) 120.
- [36] M. Beneke and Th. Feldmann, Nucl. Phys. **B592** (2001) 3.
- [37] M. Bauer, B. Stech, and M. Wirbel, Z. Phys. C **29** (1985) 637; **34** (1987) 103 .
- [38] A. Ali *et al.*, Phys. Rev. D **61** (2000) 074024; P. Ball and V. M. Braun, Phys. Rev. D **58** (1998) 094016; P. Ball *et al.*, Nucl. Phys. **B529** (1998) 323.
- [39] A. Datta and D. London, Int. J. Mod. Phys. A **19** (2004) 2505; D. London, N. Sinha, and R. Sinha, Phys. Rev. D **69** (2004) 114013; K. Abe, M. Satpathy, and H. Yamamoto, arXiv:hep-ex/0103002; I. Dunietz *et al.*, Phys. Rev. D **43** (1991) 2193.

- [40] C. M. Arnesen, Z. Ligeti, I. Z. Rothstein, and I. W. Stewart, arXiv:hep-ph/0607001; and references therein; C. M. Arnesen, I. Z. Rothstein, and I. W. Stewart, Phys. Lett. B **647** (2007) 405.
- [41] A. Datta *et al.*, Phys. Rev. D **71** (2005) 096002; A. Datta and D. London, Phys. Lett. B **595** (2004) 453.
- [42] X. Q. Li, G. R. Lu, and Y. D. Yang, Phys. Rev. D **68** (2003) 114015; **71** (2005) 019902(E); Y. H. Chen, H. Y. Cheng, and B. Tseng, Phys. Rev. D **59** (1999) 074003.
- [43] A. Ali *et al.*, arXiv:hep-ph/0703162.
- [44] A. J. Buras, P. Gambino, and U. A. Haisch, Nucl. Phys. **B570** (2000) 117.
- [45] L. Wolfenstein, Phys. Rev. Lett. **51** (1983) 1945.
- [46] J. Charles *et al.* (CKMfitter Group), Eur. Phys. J. C **41** (2005) 1; updated results and plots available at: <http://ckmfitter.in2p3.fr..>
- [47] A. Gray *et al.* (HPQCD Collaboration), Phys. Rev. Lett. **95** (2005) 212001.
- [48] P. Ball and R. Zwicky, Phys. Rev. D **71** (2005) 014015; **71** (2005) 014029; Phys. Lett. B **633** (2006) 289.
- [49] V. M. Braun, D. Y. Ivanov, and G. P. Korckemsky, Phys. Rev. D **69** (2004) 034014; A. Khodjamirian, T. Mannel, and N. Offen, Phys. Lett. B **620** (2005) 52.